



Article

Novel R2R3-MYB Transcription Factor LhMYB1 Promotes Anthocyanin Accumulation in *Lilium concolor* var. *pulchellum*

Shengnan Tian ¹, Muhammad Moaaz Ali ¹ , Mingli Ke ¹, Yuxian Lu ¹, Yiping Zheng ², Xuanmei Cai ², Shaozhong Fang ², Jian Wu ³ , Zhimin Lin ^{2,*} and Faxing Chen ^{1,*}

¹ College of Horticulture, Fujian Agriculture and Forestry University, Fuzhou 350002, China; 3210330052@fafu.edu.cn (S.T.); moaaz@fafu.edu.cn (M.M.A.); 5220330046@fafu.edu.cn (M.K.); 5220330020@fafu.edu.cn (Y.L.)

² Fujian Academy of Agricultural Sciences Biotechnology Institute, Fuzhou 350003, China; zhengyiping@faas.cn (Y.Z.); caixuanmei@faas.cn (X.C.); fangshaozhong@faas.cn (S.F.)

³ Beijing Key Laboratory of Development and Quality Control of Ornamental Crops, Department of Ornamental Horticulture, China Agricultural University, Beijing 100107, China; jianwu@cau.edu.cn

* Correspondence: linzhimin@faas.cn (Z.L.); fxchen@fafu.edu.cn (F.C.)

Abstract: *Lilium concolor* var. *pulchellum* has a brilliant flower colour, high germination rate, and resistance to cold, drought, and salinity and is an excellent source of lily germplasm. Anthocyanins are important flavonoids commonly found in plants and can make the flowers and fruits of plants more colourful. We first found that 0.2 mg/L 1-naphthaleneacetic acid (NAA) specifically induced the accumulation of anthocyanins, which were mainly cyanidins, in callus tissue culture of *Lilium*. Transcriptomic results indicated that anthocyanin accumulation was mainly involved in the flavonoid pathway, and an *LhMYB1* transcription factor encoding 267 amino acids positively associated with anthocyanin accumulation was cloned from the MYB family. Subcellular localisation in tobacco showed that the gene was located in the nucleus of epidermal cells. Virus-induced gene silencing showed that silencing of the *LhMYB1* gene on lily petals resulted in a purple to white colour change and a decrease in anthocyanin deposition, mainly in the upper and lower epidermis of the petals. Therefore, the results of this study will provide some ideas for the molecular breeding of lily flower colour.

Keywords: transcription factor; *LhMYB1*; anthocyanin accumulation; *Lilium concolor* var. *pulchellum*



Citation: Tian, S.; Ali, M.M.; Ke, M.; Lu, Y.; Zheng, Y.; Cai, X.; Fang, S.; Wu, J.; Lin, Z.; Chen, F. Novel R2R3-MYB Transcription Factor LhMYB1 Promotes Anthocyanin Accumulation in *Lilium concolor* var. *pulchellum*. *Horticulturae* **2024**, *10*, 509. <https://doi.org/10.3390/horticulturae10050509>

Academic Editors: Tetsuya Matsukawa and Daniela Scaccabarozzi

Received: 2 April 2024
Revised: 11 May 2024
Accepted: 13 May 2024
Published: 15 May 2024



Copyright: © 2024 by the authors. Licensee MDPI, Basel, Switzerland. This article is an open access article distributed under the terms and conditions of the Creative Commons Attribution (CC BY) license (<https://creativecommons.org/licenses/by/4.0/>).

1. Introduction

Anthocyanins, large secondary plant metabolites called flavonoids, are water-soluble pigments found in most vascular plants [1,2]. Anthocyanin was the common name for a group of flavonoid pigments with a hydroxylated 2-phenylchroman chromophore [3]. Anthocyanins are found in various tissues of higher plants, including flowers, fruits, seed coats, leaves, stems, tubers, and roots, and they exhibit a wide range of colours, from red to purple, blue, and black. More than 635 different anthocyanins have been identified in nature [4]. Initially, anthocyanins were naturally occurring compounds that are responsible for the colour of fruits, vegetables and plants [5]. Anthocyanins give fruits a wide range of colours, from red to purple and blue, and help to attract seed dispersers and protect them from various biotic and abiotic stresses [6]. Fruit colour is an important classification parameter as it is an indicator of ripeness, freshness, and quality [7]. Anthocyanins in fruits and vegetables are promising phytochemicals with health benefits [8]. After consumption, anthocyanins are metabolized centrally, mainly in the intestine and liver. Anthocyanins such as cornflower 3-glucoside and geraniol 3-glucoside can be absorbed in their intact form through the gastrointestinal wall and enter the systemic circulation as metabolites [9]. Anthocyanins are active against various micro-organisms, although Gram-positive bacteria are usually more susceptible to anthocyanins than Gram-negative bacteria [10]. In addition,

anthocyanins may improve cardiovascular health by reducing the risk of heart disease and stroke and have anti-carcinogenic properties that prevent cancer [11,12].

The biosynthetic pathway involves a series of enzyme-catalysed reactions to produce anthocyanins. Anthocyanins are flavonoid pigments produced via the phenylpropane pathway. The precursor and aromatic amino acid phenylalanine is mainly deaminated by phenylalanine ammonia lyase (PAL) on the outer surface of cytoplasmic and endoplasmic reticulum membranes [13]. The structural genes for anthocyanins have been characterised in many plants. They are broadly divided into two groups: upstream and downstream genes [14]. Upstream genes are those containing precursors encoding chalcone synthase (CHS), chalcone flavanone isomerase (CHI), flavanone 3-hydroxylase (F3H), and dihydroflavonol 4-reductase (DFR), which synthesise one or more of the non-anthocyanidin flavonoid pathways. Downstream, the genes are those encoding anthocyanin synthase (ANS), glycosyltransferase (GT), rhamnosyltransferase (RT), acetyltransferase (AT), and methyltransferase (MT). Finally, the anthocyanins bind to glutathione S-transferase (GST) and are effectively chelated in the vesicle [15]. At least 29 different anthocyanin forms have been identified in *Arabidopsis* [16]. To date, more than 650 different anthocyanin structures from 35 monomers have been identified as anthocyanins in nature, of which more than 90% are derived from the six most abundant anthocyanins (cornflower, delphinidin, peargonidin, malvidin, peonidin, and petunidin) [13].

Anthocyanin biosynthesis is known to be tightly regulated at the transcriptional level by the evolutionarily conserved MYB-bHLH-WD repeat sequence (MBW) complex [17]. The *c1* gene, which regulates anthocyanin biosynthesis in maize, was the first MYB transcription factor identified in plants [18]. Anthocyanin biosynthesis is normally regulated by MYB transcription factors, of which the AN2 and C1 subgroups are members. In monocots, MYB transcription factors normally regulate anthocyanin biosynthetic enzymes, together with other transcription factors [19]. In contrast, dicots have two classes of anthocyanin synthases with different TFs. Previously, two full-length R2R3-MYB cDNAs (*LhMYB6* and *LhMYB12*), which positively regulate anthocyanin biosynthesis, were isolated from the anthocyanin-accumulating perianth of the Asian hybrid lily cultivar “Montreux” [20]. *LhMYB12* is the first monocot AN2 subgroup and directly activates the chalcone synthase and dihydroflavonol 4-reductase promoters [21]. One allele of *LhMYB12*, *LhMYB12-La*, causes perianth splashing in Asian hybrid lily cv L’atvia’ [22]. *LiMYB3* may be involved in the anthocyanin biosynthesis pathway that regulates stress tolerance in tiger lily [23]. Two transcription factors of R3-MYB, *LhR3MYB1* and *LhR3MYB2*, have been identified in lily with the capacity to inhibit anthocyanin accumulation [24]. Two R2R3 MYB genes, MYB19Long and MYB19Short, have been identified in *Lilium leichtlinii*, orchid lily, and Asian hybrid lily varieties, and the spatiotemporal expression profiles of lilies were found to be closely correlated with the expression of the floral pigment biosynthesis gene in colourless protuberances [25]. In addition, the ethylene response factor LhERF4 binds directly to the promoter of *LhMYBSPLATTER* and negatively regulates the expression of key structural genes and total anthocyanin content [26]. In our study, we took advantage of the characteristics of *Lilium concolor* var. *pulchellum* callus tissues and found that NAA was able to induce anthocyanin accumulation in their callus tissues by screening with different PGRs, including GA3, IAA, picloram, and IBA. By combining transcriptomic analyses of samples under different light/dark and NAA presence/absence conditions, we identified an *LhMYB1* transcription factor among 35 MYB transcription factors associated with NAA induction. It was also confirmed that NAA induced the production of anthocyanin accumulation in callus tissue, which was mainly closely linked to the flavonoid pathway. Cloning of the *LhMYB1* gene showed that it encodes 267 amino acids. It is located in the nucleus of tobacco subcells. Silencing of the *LhMYB1* gene by VIGS showed that reduced *LhMYB1* expression could reduce anthocyanin accumulation in flower petals and occurs mainly in the upper and lower epidermis.

2. Results

2.1. Embryo Callus Induction

We used different pairs of growth PGRs to induce callus in *Lilium concolor* var. *pulchellum* on MS medium, with 0.2 mg/L NAA induction being the most typical, and it was observed that the callus tissue turned purple, and anthocyanin accumulation occurred (Figure 1A). Other PGRs, such as 0.5 mg/L picloram (Figure 1B), 0.5 mg/L IBA (Figure 1C), 0.5 mg/L GA3 (Figure 1D), 0.5 mg/L IAA (Figure 1E), and the control (Figure 1F) did not consistently induce anthocyanin accumulation throughout. From the induction of callus tissues with different concentrations of NAA, the 0.2 mg/L concentration showed the best effect on anthocyanin accumulation (Figure S1). HPLC-MS analysis showed that 0.2 mg/L NAA had the highest anthocyanin accumulation in callus tissues, whereas 1.0 mg/L NAA had the lowest (Figure S3A). In the flavonoid pathway, the expression of several structural genes was more significantly upregulated under 0.2 mg/L induction, including CHI, DFR, CHS, FLS, and F3H (Figure S3B). In addition, anthocyanin accumulation in callus tissues peaked after 15 days of induction at 0.2 mg/L (Figure S4). This was later confirmed in the anthocyanin deposition assay (Figure S5). The anthocyanin component was found to be mainly cyanidin by HPLC-MS analysis.

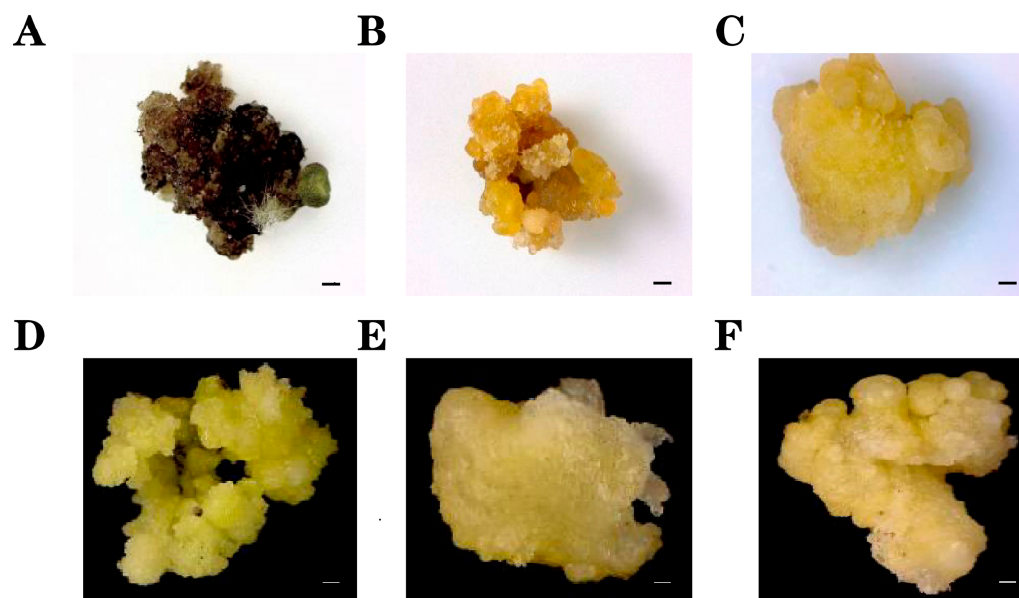


Figure 1. Induction of anthocyanin accumulation by various growth factors in lily callus tissue. (A) Induction of callus tissue by NAA. (B) Induction of callus tissue by picloram. (C) Induction of callus tissue by IBA. (D) Induction of callus tissue by GA3. (E) Induction of callus tissue by IAA. (F) Normal callus tissue growth on MS culture without exogenous PGRs. Scale = 1 cm.

2.2. Differentially Expressed Genes (DEGs)

To determine whether NAA induction of healing tissue affects anthocyanin pathways, five sets of transcriptome sequencing experiments were designed. Significant changes in differential genes occurred between several experimental groups under different treatments, including light and dark and with or without NAA (Figure 2a,b). We can see from Group A vs. Group C, Group B vs. Group E, and Group C vs. Group E that both differentially expressed genes could be enriched in the flavonoid pathway at TOP20 in the presence or absence of NAA conditions (Figure 2c,d). These results suggest that the effect of NAA on anthocyanin accumulation in lily callus tissue was mainly focused on the differential expression of flavonoid pathway genes.

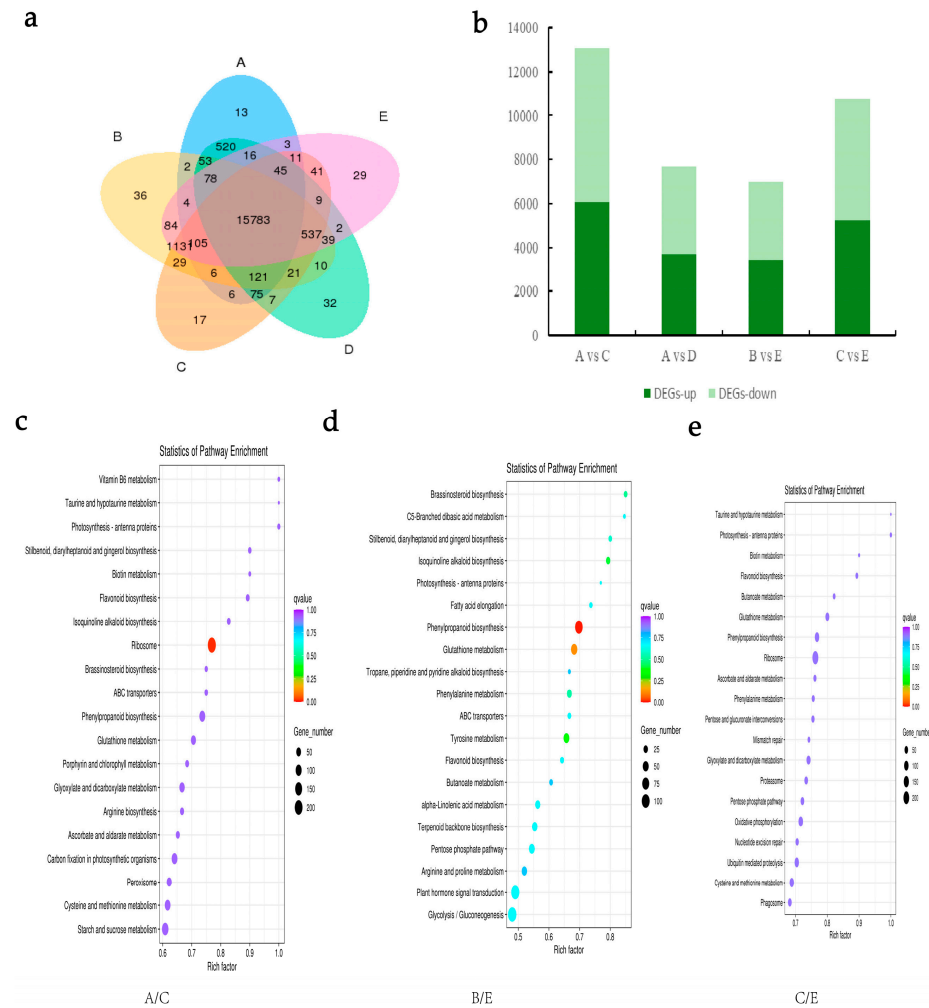


Figure 2. Transcriptome differential gene analysis and KEGG enrichment. (a) Analysis of differentially expressed genes between the five experimental groups. (b) Bar chart analysis of the up- and down-regulated genes between the five experimental groups. (c) TOP20 KEGG enrichment between A and C. (d) TOP20 KEGG enrichment between B and E. (e) TOP20 KEGG enrichment between C and E.

2.3. MYB Transcription Factor of Bioinformatics Analysis

Through transcriptome analysis, we obtained relevant transcription factors in lily and 35 differentially expressed transcription factors of the MYB family (Figure 3A,B). Structural domain analysis of LhMYB proteins revealed that most LhMYB transcription factors contain Myb-related elements such as Myb_Cef, Myb_DNA-binding, Myb_CC_LHEQLE, myb_SHAQKYF, Myb_DNA-bind_6, and so on (Figure 3C). Using cluster analysis with *Arabidopsis* MYB transcription factors, we identified an *LhMYB1* transcription factor that was closely related to *Arabidopsis* (Figure 3D). From 4.2 reverse transcribed cDNA, we cloned the full-length *LhMYB1* gene (Figure S6). Second, the results of the hormone experiments showed that the expression of LhMYB1 was higher in response to NAA than to GA3, picloram, IAA, IBA, and NAA + picloram (Figure S7A,B). Among the different concentrations of NAA, consistent with the anthocyanin accumulation content, the highest expression of *LhMYB1* was found at 0.2 mg/L (Figure S7C). In 0.2 mg/L NAA-induced callus tissue, *LhMYB1* expression increased with time in the light (Figure S7D).

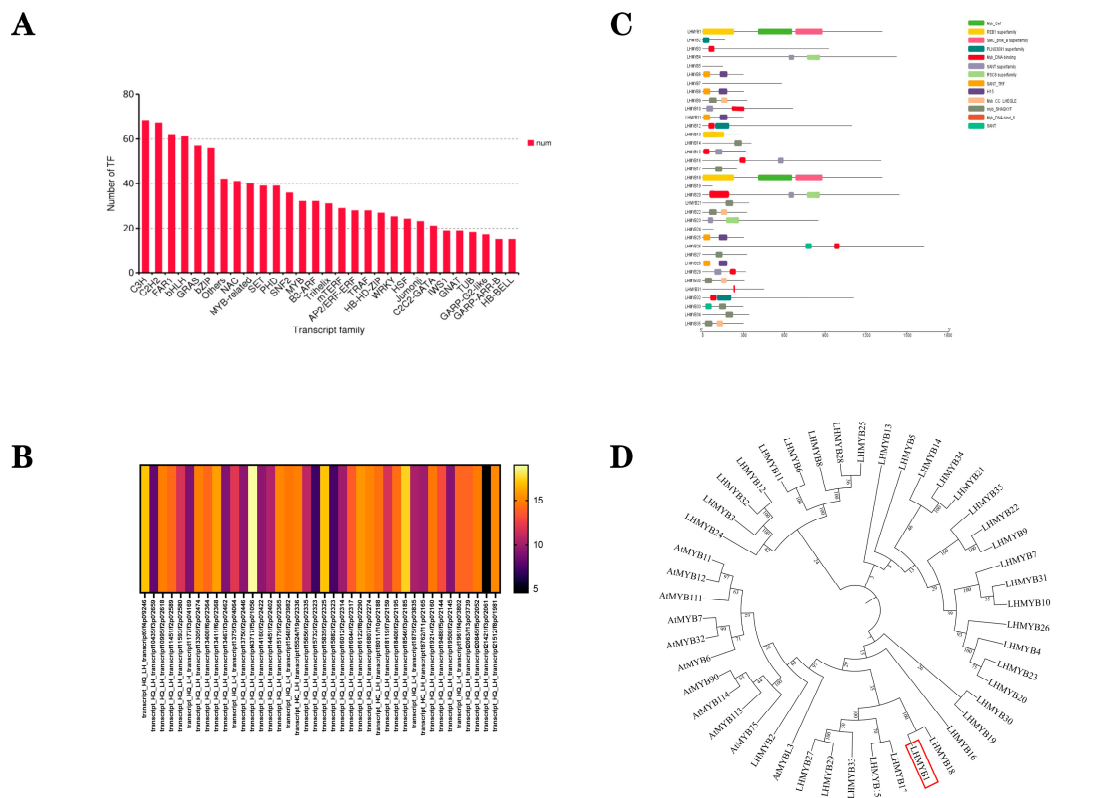


Figure 3. Analysis of biological information of MYB transcription factors in *Lilium*. (A) Analysis of the distribution of transcription factors in *Lilium*. (B) Differential expression analysis of MYB transcription factors. (C) Protein structure analysis of 35 MYB transcription factors. (D) Cluster analysis of MYB transcription factors in *Lilium* with *Arabidopsis thaliana*. The target gene LhMYB1 is represented by the red marker box.

2.4. Subcellular Localization of LhMYB1

To understand the functional location of the different *LhMYB1* genes, the subcellular localisation of the LhMYB1 protein was visualised using GFP fusions. The LhMYB1:GFP fusion protein drives the CaMV 35S promoter in transient expression assays using tobacco leaves. As shown in Figure 4A, confocal observation revealed fluorescent signals of all LhMYB1:GFP proteins in the nuclei. This was in complete agreement with the DAPI staining results. It was clear that the localisation of 35S:gfp in tobacco took place in different organelles (Figure 4B).

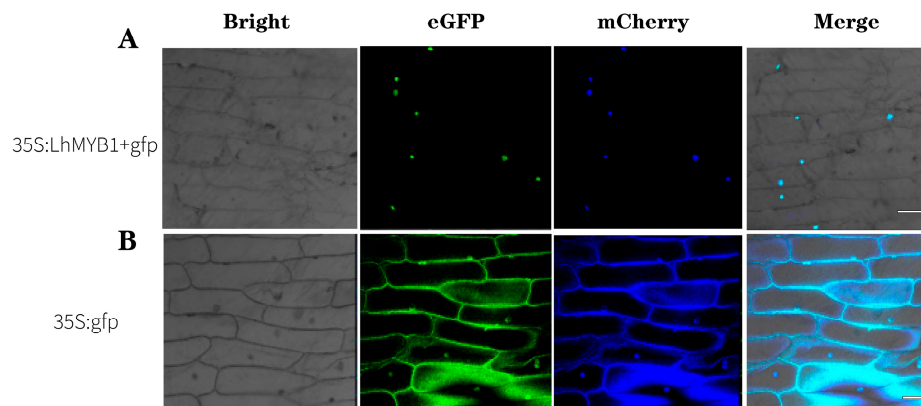


Figure 4. Subcellular localisation of LhMYB1 proteins in tobacco. (A) Subcellular localisation of the LhMYB1 protein in tobacco epidermal cells; scale bar: 50 µm. (B) Subcellular localisation of the GFP protein in tobacco epidermal cells; scale bar: 50 µm.

2.5. Virus-Induced Gene Silencing in *Lilium* Petals

To elucidate the role of *LhMYB1* in anthocyanin accumulation, we used VIGS to knock out the *LhMYB1* gene in lily petals and observed changes in flower colour. For gene silencing, we amplified a 226 bp fragment of the full length of *LhMYB1*. When the vacuum-infiltrated petals were exposed to light for 7 days, we could clearly see a whitening of the petal colour compared to the control (Figure 5A). Relative quantitative expression analysis of the *LhMYB1* gene showed that the gene was significantly downregulated after silencing compared to the control (Figure 5B). Meanwhile, RT-PCR assays for CP protein in TRV1 and MP protein in TRV2 indicated successful *Agrobacterium* infection (Figure 5C). Observation of the pigment distribution of petal epidermal cells using light microscopy showed that TRV silencing of the *LhMYB1* gene caused a decrease in pigmentation mainly in the upper and lower epidermis of the petals, while the effect on spot pigmentation was not obvious (Figure 5C).

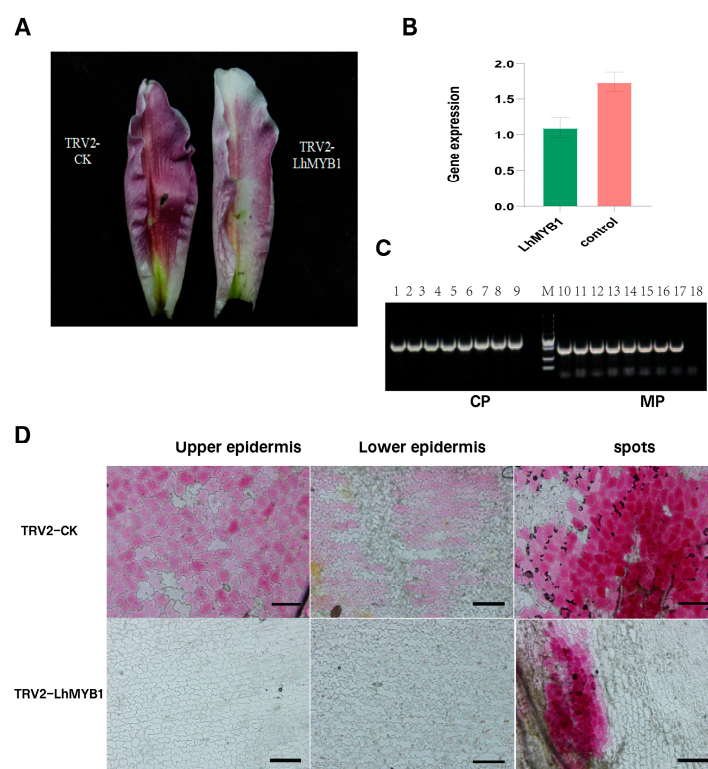


Figure 5. Establishment of a petal VIGS system for the *LhMYB1* gene and analysis of the assay in *Lilium*. (A) Petal status after 7 days of mixed infection with TRV1/TRV2 and TRV1/ TRV2-*LdSERK1*. (B) Relative quantitative analysis of the expression of *LhMYB1* on the petals of TRV2-CK and TRV2-*LhMYB1* for 11 days after *Agrobacterium* infection. (C) CP and MP on TRV1 and TRV2 /TRV2-*LhMYB1* backbones in petals of both treatment groups were detected as 226 bp transcript segments. CP: coat protein, MP: movement protein. Numbers 1–4 refer to TRV1/TRV2; 5–8 refer to TRV1/TRV2-*LdSERK1*; 9 refers to negative; 10–13 refer to TRV1/TRV2; 14–17 refer to TRV1/TRV2-*LdSERK1*; 18 refers to negative. (D) Morphology of anthocyanin deposition in the petal epidermis under light microscopy, including upper epidermis, lower epidermis, and spots of TRV2-CK and TRV-*LhMYB1*. Scale = 200 μ m.

3. Discussion

Anthocyanins are water-soluble flavonoid pigments that belong to the five major classes of plant pigments and have a wide range of biological activities, including antioxidant, anti-inflammatory, and anti-cancer properties [27]. Typically synthesised mainly in the epidermis and flesh of the fruit, anthocyanins have an attractive reddish-purple colour and regulating anthocyanin levels has a positive effect on fruit quality [28]. Anthocyanins,

which are mainly found in the midrib and pericarp, also determine the colour of cereal grains [29]. Anthocyanins are the main compounds responsible for flower colour and are present in more than 90% of angiosperms, and anthocyanin accumulation has now been extensively studied in most model and horticulturally important plants [30], including *Arabidopsis thaliana* [31], tomato [32], pear [33], apple [34], petunia [35], and so on. There has been some research on anthocyanins in lilies, mainly focusing on the floral organ. This study focuses on the accumulation of anthocyanins from the callus tissue induction process of *Lilium concolor* var. *pulchellum* and analyses the molecular mechanism of anthocyanin formation from a different perspective.

Firstly, the application of some phytohormones and signalling molecules will stimulate the synthesis of endogenous anthocyanins [36]. Light, ethylene response factors (ERFs) and plant growth factors are the main regulators of anthocyanin synthesis. Light induces the expression of PpbHLH64 and the accumulation of anthocyanins in the callus tissues of pear fruit, mainly because its overexpression causes callus tissues to show an enhanced red colour under light conditions [37]. In Lycium fruit, ABA accumulation will stimulate transcription of the MYB-bHLH-WD40 transcription factor complex and cause upregulation of the expression of structural genes involved in flavonoid biosynthesis, thereby promoting anthocyanin production [38]. It has been shown that DELLA, a negative inhibitor of the GA signalling pathway, is an essential regulator of the accumulation of anthocyanins induced by nitrogen deficiency [39]. In *Salvia miltiorrhiza*, MeJA negatively regulates the transcription factor GmbHLH60 and inhibits anthocyanin biosynthesis by repressing the structural genes SmTAT1 and SmDFR [40]. Brassinolide, via MdBHE2.2-MdMYB60, reduces flavonoid and anthocyanin content in apple seedlings and callus tissues [41]. In many fruits, ethylene is the key to ripening-induced anthocyanin production. The redox state of the plastoquinone (PQ) pool of the PET chain, together with the phytohormone ethylene and phytohormone-like sugars, regulates anthocyanin biosynthesis genes [42]. Growth factors play an important role in helping plant growth and development. The regulatory effects of growth PGRs on anthocyanin accumulation are not well understood. In apple, the growth hormone-related *MdIAA26* gene is degraded by growth hormone induction, and overexpression of this gene promotes anthocyanin accumulation in apple callus tissue [43]. Overexpression of *MdIAA121* and *MdARF13* in transgenic callus tissues of red apple attenuated the inhibitory effect of *MdARF13* on anthocyanin biosynthesis [44]. Our study showed that NAA can promote anthocyanin accumulation in lily callus tissue, and 0.2 mg/L was found to be the optimal induction concentration (Figure S3). In sweet cherry fruit, treatment with NAA induces ripening by altering ethylene production, which in turn increases anthocyanin production through ABA metabolism [45]. In our study, exogenous NAA treatment was mainly responsible for the upregulation of endogenous NAA levels. The results suggest that 2,4-D, NAA and IAA control anthocyanin biosynthesis by regulating the expression of TT8, GL3, and PAP1, as well as genes in the anthocyanin biosynthetic pathway such as DFR and ANS [46].

Phytochrome-interacting factors (PIFs) are involved in environmentally induced anthocyanin biosynthesis by interacting with the MYB-bHLH-WD40 (MBW) complex [47]. Most plant MYB proteins contain two incomplete MYB repeat sequences. *Arabidopsis* has about 339 MYB genes [48]. In strawberry, 111 MYBs (of which 105 are R2R3 MYBs) and 61 MYB-associated transcription factors have been identified [49]. Analysis of the transcriptome sequencing data in this study showed that 35 MYBs and 36 MYB-associated transcription factors were identified in *Lilium concolor* var. *pulchellum*. Through cluster analysis, combined with analysis of MYB expression in response to different PGRs and different concentrations of NAA, we finally selected an *LhMYB1* gene encoding 267 amino acids. It was homologous to AtMYBL3 in *Arabidopsis* and AtMYB11 had been reported to be related to anthocyanins (Figure 3D). Certainly, this is the first report in lily that 1-naphthaleneacetic acid (NAA) induces the accumulation of anthocyanins, while MYB responds to it. Meanwhile, the results showed that the *LhMYB1* expression levels increased in response to anthocyanin accumulation (Figure S7). In addition, the results of TRV-LhMYB1

on lily petals showed that silencing the LhMYB1 gene on petals would reduce flower colour and that anthocyanin degradation occurred mainly in the upper and lower epidermal parts.

4. Materials and Methods

4.1. Plant Materials and Growth Conditions

Lily varieties of *Lilium concolor* var. *Pulchellum* were grown at the Germplasm Resource Nursery of Yanping District, Nanping City, Fujian Province, China. Callus tissues were induced in MS medium (with the addition of 1.0 mg/L picloram+6-BA 0.2 mg/L+2.4-D 0.5 mg/L) under dark conditions at 27 °C using lily scales as explants. We also had selected various exogenous PGRs to induce callus, including NAA, picloram, GA3, IBA, NAA+picloram, and different concentrations of NAA. Anthocyanin accumulation was also observed at various times during callus induced with 0.2 mg/L NAA. The anthocyanin induction experiments were divided into five groups for the transcriptome: (A) growth on light culture-inducing medium without NAA; (B) growth on dark culture-inducing medium without NAA; (C) growth on light culture-inducing medium with 0.1 mg/L NAA; (D) 0.1 mg/L NAA light culture growth and then transfer to dark culture; and (E) 0.1 mg/L NAA dark culture growth and then transfer to light culture.

4.2. Sample Extraction and Analysis of Anthocyanin Components

NAA-induced callus tissue and control tissue were each weighed (5 g) for the experiment. It was rapidly ground and crushed in liquid nitrogen and then extracted by stirring with 0.1 M/L hydrochloric acid at a solid–liquid ratio of 1:20. The extraction was assisted by an ultrasonic bath with an ultrasonic power of 250 W. The water temperature in the bath was controlled at 25 °C and the samples were extracted for 40 min. Impurities were removed by filtering through a 0.45 µm membrane and extracted twice using equal volumes of light petroleum and ethyl acetate. HPLC analysis was performed on an HPLC 1200 (Agilent Technologies, Santa Clara, CA, USA), equipped with an Agilent 1200 HPLC variable wavelength detector. The SB-C18 chromatographic column (4.6 mm × 250 mm, 5 µm, Agilent Technologies, Howard County, MD, USA) was selected and the sample was injected in a volume of 20 µL, with mobile phase A being an aqueous solution of 1% formic acid and mobile phase B being a 100% acetonitrile solution at a flow rate of 0.25 mL/min. The gradient program is described as follows: 0–5 min, 90–60% B; 5–9 min, 60% B; 9–17 min, 60–10% B; 17–18 min, 90% B; 18–19 min, 10% B; 19–20 min, 10% B. The low-resolution electrospray mass spectrometry was conducted using a solarix ion trap mass spectrometer (MS) (Bruker Daltonics, Billerica, MA, USA) [50]. Analyses were performed by LC-QTOF (Santa Clara, CA, USA, Agilent 6545B) at 530 nm using delphinidin, cyanidin, petunidin, pelargonin, and mallow pigments as standards [51]. The anthocyanin accumulated in the samples was cyanidin (Figure S2).

4.3. Total RNA Extraction and Transcriptome Sequencing

For each of the four treated samples, 100 mg of callus was collected and ground with liquid nitrogen. Total RNA was extracted according to the instructions of the RNA extraction kit (Beijing, China, TIANGEN, DP441). The quality of the RNA was determined by 1% agarose gel electrophoresis and the depth and purity of the RNA was assessed by ultra-micro detector (USA, Thermo, Nanodrop) to further purify the qualified total RNA. The cDNA library construction and high-throughput sequencing were performed by Novogene (Tianjin, China). The full-length transcriptome was based on the PacBio Sequel triple sequencing platform, which directly obtained the complete transcript, including the 5', 3' UTR and polyA tails without splicing interruption. Construction of a full-length transcriptome library was performed using oligo (dT) magnetic bead enrichment. The two core components of PacBio SMRT Iso-seq sequencing were the structural analysis of transcripts and the significance analysis of gene expression differences.

4.4. Analysis of Differentially Expressed Genes (DEGs)

The FPKM method was used to calculate the expression level of each of the annotated genes. Using DESeq2 package, the resulting gene expression levels were subjected to a DEG screen between samples from groups A, B, C, and D. Screening thresholds were $|\log_2(\text{fold change})| > 1$ and $p\text{-value} < 0.05$. The smaller the p value, the more significant the difference in gene expression. In addition, GO and KEGG enrichment of DEGs was analysed. Goseq R package and KOBAS 2.0 software packages were used.

4.5. Fluorescence Quantitative PCR for Verification of Gene Expression

RT-qPCR was used for gene and differential gene expression analysis. Primers were designed using Primer 6.0 software, cDNA synthesis was used as a template, and *Lilium × formolongi* EF-1a was used as an internal reference gene. Quantitative real-time PCR was performed using the AceQ Universal SYBR qPCR Master Mix Kit (Nazyme, Nanjing, China). The reaction system (10 μ L) consisted of 100 ng cDNA as template, 0.4 μ L of each gene-specific primer (10 pmol/L), 5.5 μ L SYBR Green Supermix, and sufficient ddH₂O. The reaction procedure was 95 °C pre-denaturation for 2 min, 95 °C denaturation for 10 s, 61 °C annealing for 1 min, 40 cycles, 95 °C denaturation for 10 s, 60 °C annealing for 30 s, and 97 °C for 1 s to generate a solution curve. Three replicates were performed for each sample. The relative quantitative expression of genes was calculated as $2^{-\Delta\Delta CT}$. Statistical analysis of the data was performed using SPSS 20.0 software.

4.6. Cloning of the LhMYB1 Gene

The cDNA extracted in 4.2 was used as an amplification template. A pair of primers, MYBF and MYBR, were designed using the LhMYB1 cDNA sequence predicted from the transcriptome data. PCR amplification was performed using Phanta HS Super-Fidelity DNA Polymerase (Vazyme, Nanjing, China) in a total volume of 20 μ L. The PCR reaction conditions used were as follows: initial denaturation at 98 °C for 2 min; 35 cycles of denaturation at 98 °C for 15 s, annealing at 58 °C for 30 s, and extension at 72 °C for 1 min; and a final extension at 72 °C for 5 min. Gene fragments were purified using a PCR purification test kit (TIANGEN, Beijing, China) and cloned into pGXT vector. *E. coli*-positive clones were selected. A 954 bp putative LhMYB1 fragment was cloned.

4.7. Vector Construction and Agrobacterium Transformation

A 225 bp fragment was amplified from the cDNA template in 4.2 using TRV-LhMYB1F and TRV-LhMYB1R primers. This empty vector TRV2 was linearised with *Eco*RI and *Xho*I, and the small fragment of the LhMYB1 gene inserted into TRV2 was transformed into *Agrobacterium* GV3101 strain. In addition, the pCAMBIA1302 plasmid was digested with *Kpn*I and *Bam*HI. This full-length fragment of the LhMYB1 gene was seamlessly cloned into the vector (Vazyme, Technology Co., Ltd., Nanjing, China), which is named as pCAMBIA1302-LhMYB1.

4.8. Establishment of the VIGS Gene Silencing System in Lily Petals

The TRV and TRV2-LhMYB1 clones of *Agrobacterium tumefaciens* were isolated and grown in the dark at 200 rpm for 18 h at 28 °C until the OD₆₀₀ of the bacterial solution was approximately 0.8 and were then collected by centrifugation at 5000 rpm for 10 min. A suspension (1M MgCl₂, 200 μ M acetosyringone and 1M 2-(N morpholino) ethane sulfonic acid) was used and resuspended to an OD₆₀₀ of 1.0 with pH 5.6, and TRV1, TRV2, and TRV2-LhMYB1 were mixed in equal volumes 1:1 and allowed to stand in the dark for 3 h before transformation by vacuum osmosis infiltration. The group infected with the *Agrobacterium tumefaciens* mixture of TRV1 and TRV2 was used as a control. The middle petal of the bud was taken as infestation material and cleaned, and then small holes were made with a needle to increase the infestation efficiency. The petals were then dipped in the infestation solution and pressed under vacuum at 0.8 Kpa for 15 min and finally placed on MS medium and cultured in the dark at 27 °C for 2 days and transferred to light for 7 days.

4.9. Subcellular Localization in Tobacco

The pCAMBIA1302 and pCAMBIA1302-LhMYB1 *Agrobacterium* clones were isolated and grown in the dark at 28 °C, 200 rpm until the OD₆₀₀ of the bacterial solution was approximately 0.8, and the supernatant was discarded after centrifugation. The bacterial culture grown overnight (5 mL) was used to inoculate 40 mL of YEB medium supplemented with 800 µL buffer containing 1 M MgCl₂ + 200 µM AS + 1 M MES, pH 5.6. The cells were harvested by centrifugation and resuspended to a final concentration corresponding to an absorbance of 1.0 at 600 nm for 3 h in the dark at 28 °C. Young apical leaves (5–6 leaves) were infiltrated with recombinant *Agrobacterium* strains using a syringe (2 mL) without a needle. Pins were used to damage the leaf surface to improve penetration. An *Agrobacterium* strain containing pCAMBIA1302 was used as a control. Leaves were photographed at 36 to 48 h after infiltration for confocal observation. DAPI staining solution was used as a positive control.

4.10. Statistical Analysis

The interference efficiency of dsRNA at different time points was tested by independent samples *t*-test. The significance level was tested using $p < 0.05$.

5. Conclusions

Lilium concolor var. *Pulchellum* is a variety of Wodan lily, which is found in many parts of China. It is adaptable and cold tolerant, has a high embryo rate, and is often used to improve hybrid varieties. In our study, NAA was found to cause an accumulation of anthocyanins during the callus tissue culture stage of the lily. This provides us with good research material to unravel the interaction between growth hormone and anthocyanin deposition in lilies. Combined with transcriptome analysis, cloning of the *LhMYB1* gene further reveals that while the *LhMYB1* gene responds positively to NAA, its increased expression promotes the accumulation of anthocyanins in callus tissues, which is also verified by VIGS silencing of petals. Previously, we had preliminary data (unpublished) showing that upregulation of the transcription factor LhMYB1 was the most important factor in upregulating the expression of LhDFR. For this reason, we are going to focus on whether the transcription factor LhMYB1 is involved in the regulation of the transcription process of the LhDFR gene. In this way, we will elucidate a new regulatory network of anthocyanin biosynthesis in lily. In conclusion, these molecular mechanisms and physiological and biochemical studies will provide theoretical references for the next step in molecular breeding of lily flower colour. For example, we can use novel gene editing techniques to mutate target genes in order to change the colour of a flower. Moreover, bioreactors can now be used for efficient large-scale callus tissue culture. This can lead to industrialised production and extraction of anthocyanins. In addition, *Lilium concolor* var. *Pulchellum* pigment is a flavonoid pigment with increased hair longevity and reduction resistance and also has good prospects for development and application in the food industry.

Supplementary Materials: The following supporting information can be downloaded at: <https://www.mdpi.com/article/10.3390/horticulturae10050509/s1>. Figure S1. Different concentrations of NAA induced the accumulation of anthocyanins in the callus tissue. Figure S2. Testing and analysing anthocyanins in lilies. Figure S3. Extraction analysis of anthocyanins and gene expression analysis of the pathways involved in flavonoid metabolism. Figure S4. Phenotypic observation of 0.2 mg/L NAA induced healing tissues at different times. Figure S5. Determination of anthocyanin deposition by 0.2 mg/L NNAA during induction of lily callus tissue in different time by HPLC. Figure S6. Cloning of LhMYB1 gene. Figure S7. Analysing the relative quantitative expression of LhMYB1 under varying conditions. Table S1. List of gene-specific primers used for gene cloning.

Author Contributions: Conceptualization, S.T. and Z.L.; methodology, S.T. and J.W.; software, Y.L.; validation, M.K.; formal analysis, Y.Z. and X.C.; investigation, S.T.; resources, S.F. and Z.L.; data curation, Z.L. and S.T.; writing—original draft preparation, Z.L. and S.T.; writing—review and editing,

M.M.A., Z.L. and F.C.; visualization, S.T.; supervision, Z.L. and F.C.; project administration, Z.L.; funding acquisition, Z.L. All authors have read and agreed to the published version of the manuscript.

Funding: This research was funded by the Fujian Academy of Agricultural Sciences Foreign Cooperation Project (DWHZ2024-10), Basic Research Projects of Fujian Provincial Public Welfare Research Institutes (2022R1027007), and the Forestry Science and Technology Project in Fujian Province (ZMGG-0711).

Data Availability Statement: Data are contained within the article and Supplementary Materials.

Acknowledgments: We are very grateful to Wu Jian's team from China Agricultural University for their support in providing VIGS vector plasmids.

Conflicts of Interest: The authors declare no conflicts of interest.

References

- Delgado-Vargas, F.; Jiménez, A.R.; Paredes-López, O. Natural pigments: Carotenoids, anthocyanins, and betalains—characteristics, biosynthesis, processing, and stability. *Crit. Rev. Food Sci. Nutr.* **2000**, *40*, 173–289. [[CrossRef](#)] [[PubMed](#)]
- Alappat, B.; Alappat, J. Anthocyanin Pigments: Beyond Aesthetics. *Molecules* **2020**, *25*, 5500. [[CrossRef](#)] [[PubMed](#)]
- Yoshida, K.; Mori, M.; Kondo, T. Blue flower color development by anthocyanins: From chemical structure to cell physiology. *Nat. Prod. Rep.* **2009**, *26*, 884–915. [[CrossRef](#)] [[PubMed](#)]
- Glover, B.J.; Martin, C. Anthocyanins. *Curr Biol.* **2012**, *22*, R147–R150. [[CrossRef](#)] [[PubMed](#)]
- Kong, J.-M.; Chia, L.-S.; Goh, N.-K.; Chia, T.-F.; Brouillard, R. Analysis and biological activities of anthocyanins. *Phytochemistry* **2003**, *64*, 923–933. [[CrossRef](#)] [[PubMed](#)]
- Zhao, Y.; Sun, J.L.; Cherono, S.; An, J.-P.; Allan, A.C.; Han, Y.P. Colorful hues: Insight into the mechanisms of anthocyanin pigmentation in fruit. *Plant Physiol.* **2023**, *192*, 1718–1732. [[CrossRef](#)]
- Kapoor, L.; Simkin, A.; Doss, C.G.P.; Siva, R. Fruit ripening: Dynamics and integrated analysis of carotenoids and anthocyanins. *BMC Plant Biol.* **2022**, *22*, 27. [[CrossRef](#)]
- Mattoo, A.K.; Dwivedi, S.L.; Dutt, S.; Singh, B.; Garg, M.; Ortiz, R. Anthocyanin-Rich Vegetables for Human Consumption—Focus on Potato, Sweetpotato and Tomato. *Int. J. Mol. Sci.* **2022**, *23*, 2634. [[CrossRef](#)] [[PubMed](#)]
- Fang, J. Bioavailability of anthocyanins. *Drug Metab. Rev.* **2014**, *46*, 508–520. [[CrossRef](#)]
- Cisowska, A.; Wojnicz, D.; Hendrich, A.B. Anthocyanins as antimicrobial agents of natural plant origin. *Nat. Prod. Commun.* **2011**, *6*, 149–156. [[CrossRef](#)]
- Gonzali, S.; Perata, P. Anthocyanins from Purple Tomatoes as Novel Antioxidants to Promote Human Health. *Antioxidants* **2020**, *9*, 1017. [[CrossRef](#)] [[PubMed](#)]
- Khoo, H.E.; Azlan, A.; Tang, S.T.; Lim, S.M. Anthocyanidins and anthocyanins: Colored pigments as food, pharmaceutical ingredients, and the potential health benefits. *Food Nutr. Res.* **2017**, *61*, 1361779. [[CrossRef](#)] [[PubMed](#)]
- Chaves-Silva, S.; Santos, A.L.D.; Chalfun-Júnior, A.; Zhao, J.; Peres, L.E.P.; Benedito, V.A. Understanding the genetic regulation of anthocyanin biosynthesis in plants—Tools for breeding purple varieties of fruits and vegetables. *Phytochemistry* **2018**, *153*, 11–27. [[CrossRef](#)] [[PubMed](#)]
- Shoeva, O.Y.; Glagoleva, A.Y.; Khlestkina, E.K. The factors affecting the evolution of the anthocyanin biosynthesis pathway genes in monocot and dicot plant species. *BMC Plant Biol.* **2017**, *17*, 256. [[CrossRef](#)] [[PubMed](#)]
- Mueller, L.A.; Goodman, C.D.; Silady, R.A.; Walbot, V. AN9, a petunia glutathione S-transferase required for anthocyanin sequestration, is a flavonoid-binding protein. *Plant Physiol.* **2000**, *123*, 1561–1570. [[CrossRef](#)]
- Shi, M.-Z.; Xie, D.-Y. Biosynthesis and metabolic engineering of anthocyanins in *Arabidopsis thaliana*. *Recent Pat. Biotechnol.* **2014**, *8*, 47–60. [[CrossRef](#)]
- Sun, C.L.; Deng, L.; Du, M.M.; Zhao, J.H.; Chen, Q.; Huang, T.T.; Jiang, H.L.; Li, C.-B.; Li, C.Y. A Transcriptional Network Promotes Anthocyanin Biosynthesis in Tomato Flesh. *Mol. Plant* **2020**, *13*, 42–58. [[CrossRef](#)] [[PubMed](#)]
- Ma, D.; Constabel, C.P. MYB Repressors as Regulators of Phenylpropanoid Metabolism in Plants. *Trends Plant Sci.* **2019**, *24*, 275–289. [[CrossRef](#)]
- Yan, H.L.; Pei, X.N.; Zhang, H.; Li, X.; Zhang, X.X.; Zhao, M.H.; Chiang, V.L.; Sederoff, R.R.; Zhao, X.Y. MYB-Mediated Regulation of Anthocyanin Biosynthesis. *Int. J. Mol. Sci.* **2021**, *22*, 3103. [[CrossRef](#)]
- Yamagishi, M.; Shimoyamada, Y.; Nakatsuka, T.; Masuda, K. Two R2R3-MYB genes, homologs of Petunia AN2, regulate anthocyanin biosyntheses in flower Tepals, tepal spots and leaves of asiatic hybrid lily. *Plant Cell Physiol.* **2010**, *51*, 463–474. [[CrossRef](#)]
- Lai, Y.-S.; Shimoyamada, Y.; Nakayama, M.; Yamagishi, M. Pigment accumulation and transcription of LhMYB12 and anthocyanin biosynthesis genes during flower development in the Asiatic hybrid lily (*Lilium* spp.). *Plant Sci.* **2012**, *194*, 136–147. [[CrossRef](#)] [[PubMed](#)]
- Yamagishi, M.; Toda, S.; Tasaki, K. The novel allele of the LhMYB12 gene is involved in splatter-type spot formation on the flower tepals of Asiatic hybrid lilies (*Lilium* spp.). *New Phytol.* **2014**, *201*, 1009–1020. [[CrossRef](#)] [[PubMed](#)]

23. Yong, Y.B.; Zhang, Y.; Lyu, Y.M. A MYB-Related Transcription Factor from *Lilium lancifolium* L. (LlMYB3) Is Involved in Anthocyanin Biosynthesis Pathway and Enhances Multiple Abiotic Stress Tolerance in *Arabidopsis thaliana*. *Int. J. Mol. Sci.* **2019**, *20*, 3195. [[CrossRef](#)]
24. Sakai, M.; Yamagishi, M.; Matsuyama, K. Repression of anthocyanin biosynthesis by R3-MYB transcription factors in lily (*Lilium* spp.). *Plant Cell Rep.* **2019**, *38*, 609–622. [[CrossRef](#)] [[PubMed](#)]
25. Yamagishi, M. Isolation and identification of MYB transcription factors (MYB19Long and MYB19Short) involved in raised spot anthocyanin pigmentation in lilies (*Lilium* spp.). *J. Plant Physiol.* **2020**, *250*, 153164. [[CrossRef](#)]
26. Cao, Y.-W.; Song, M.; Bi, M.-M.; Yang, P.-P.; He, G.-R.; Wang, J.; Yang, Y.; Xu, L.-F.; Ming, J. Lily (*Lilium* spp.) LhERF4 negatively affects anthocyanin biosynthesis by suppressing LhMYBSPLATTER transcription. *Plant Sci.* **2024**, *342*, 112026. [[CrossRef](#)] [[PubMed](#)]
27. Chen, B.-H.; Inbaraj, B.S. Nanoemulsion and Nanoliposome Based Strategies for Improving Anthocyanin Stability and Bioavailability. *Nutrients* **2019**, *11*, 1052. [[CrossRef](#)]
28. Jezek, M.; Zörb, C.; Merkt, N.; Geilfus, C.-M. Anthocyanin Management in Fruits by Fertilization. *J. Agric. Food Chem.* **2018**, *66*, 753–764. [[CrossRef](#)] [[PubMed](#)]
29. Zykin, P.A.; Andreeva, E.A.; Lykholay, A.N.; Tsvetkova, N.V.; Voylovkov, A.V. Anthocyanin Composition and Content in Rye Plants with Different Grain Color. *Molecules* **2018**, *23*, 948. [[CrossRef](#)]
30. Ye, L.-J.; Möller, M.; Luo, Y.-H.; Zou, J.-Y.; Zheng, W.; Wang, Y.-H.; Liu, J.; Zhu, A.-D.; Hu, J.-Y.; Li, D.-Z.; et al. Differential expressions of anthocyanin synthesis genes underlie flower color divergence in a sympatric *Rhododendron sanguineum* complex. *BMC Plant Biol.* **2021**, *21*, 204. [[CrossRef](#)]
31. Trinh, C.S.; Jeong, C.Y.; Lee, W.J.; Truong, H.A.; Chung, N.; Han, J.; Hong, S.-W.; Lee, H. *Paenibacillus pabuli* strain P7S promotes plant growth and induces anthocyanin accumulation in *Arabidopsis thaliana*. *Plant Physiol. Biochem.* **2018**, *129*, 264–272. [[CrossRef](#)]
32. Li, N.; Wu, H.; Ding, Q.Q.; Li, H.H.; Li, Z.F.; Ding, J.; Li, Y. The heterologous expression of *Arabidopsis* PAP2 induces anthocyanin accumulation and inhibits plant growth in tomato. *Funct. Integr. Genom.* **2018**, *18*, 341–353. [[CrossRef](#)]
33. Song, L.Y.; Wang, X.L.; Han, W.; Qu, Y.Y.; Wang, Z.G.; Zhai, R.; Yang, C.Q.; Ma, F.W.; Xu, L.F. PbMYB120 Negatively Regulates Anthocyanin Accumulation in Pear. *Int. J. Mol. Sci.* **2020**, *21*, 1528. [[CrossRef](#)] [[PubMed](#)]
34. Zhao, S.S.; Blum, J.A.; Ma, F.F.; Wang, Y.Z.; Borejsza-wysocka, E.; Ma, F.W.; Cheng, L.L.; Li, P.M. Anthocyanin Accumulation Provides Protection against High Light Stress While Reducing Photosynthesis in Apple Leaves. *Int. J. Mol. Sci.* **2022**, *23*, 12616. [[CrossRef](#)] [[PubMed](#)]
35. Ai, T.N.; Naing, A.H.; Arun, M.; Lim, S.-H.; Kim, C.K. Sucrose-induced anthocyanin accumulation in vegetative tissue of *Petunia* plants requires anthocyanin regulatory transcription factors. *Plant Sci.* **2016**, *252*, 144–150. [[CrossRef](#)] [[PubMed](#)]
36. Ahammed, G.J.; Yang, Y.X. Anthocyanin-mediated arsenic tolerance in plants. *Environ. Pollut.* **2022**, *292*, 118475. [[CrossRef](#)] [[PubMed](#)]
37. Tao, R.Y.; Yu, W.J.; Gao, Y.H.; Ni, J.B.; Yin, L.; Zhang, X.; Li, H.X.; Wang, D.S.; Bai, S.L.; Teng, Y.W. Light-Induced Basic/Helix-Loop-Helix64 Enhances Anthocyanin Biosynthesis and Undergoes CONSTITUTIVELY PHOTOMORPHOGENIC1-Mediated Degradation in Pear. *Plant Physiol.* **2020**, *184*, 1684–1701. [[CrossRef](#)] [[PubMed](#)]
38. Li, G.; Zhao, J.H.; Qin, B.B.; Yin, Y.; An, W.; Mu, Z.X.; Cao, Y.L. ABA mediates development-dependent anthocyanin biosynthesis and fruit coloration in *Lycium* plants. *BMC Plant Biol.* **2019**, *19*, 317. [[CrossRef](#)]
39. Zhang, Y.Q.; Liu, Z.J.; Liu, J.P.; Lin, S.; Wang, J.F.; Lin, W.X.; Xu, W.F. GA-DELTA pathway is involved in regulation of nitrogen deficiency-induced anthocyanin accumulation. *Plant Cell Rep.* **2017**, *36*, 557–569. [[CrossRef](#)]
40. Liu, S.C.; Wang, Y.; Shi, M.; Maoz, I.; Gao, X.K.; Sun, M.H.; Yuan, T.P.; Li, K.L.; Zhou, W.; Guo, X.H.; et al. SmbHLH60 and SmMYC2 antagonistically regulate phenolic acids and anthocyanins biosynthesis in *Salvia miltiorrhiza*. *J. Adv. Res.* **2022**, *42*, 205–219. [[CrossRef](#)]
41. Wang, Y.C.; Mao, Z.L.; Jiang, H.Y.; Zhang, Z.Y.; Wang, N.; Chen, X.S. Brassinolide inhibits flavonoid biosynthesis and red-flesh coloration via the MdBEH2.2-MdMYB60 complex in apple. *J. Exp. Bot.* **2021**, *72*, 6282–6399. [[CrossRef](#)] [[PubMed](#)]
42. Das, P.K.; Geul, B.; Choi, S.-B.; Yoo, S.-D.; Park, Y.-I. Photosynthesis-dependent anthocyanin pigmentation in *Arabidopsis*. *Plant Signal. Behav.* **2011**, *6*, 23–25. [[CrossRef](#)] [[PubMed](#)]
43. Wang, C.-K.; Han, P.-L.; Zhao, Y.-W.; Ji, X.-L.; Yu, J.-Q.; You, C.-X.; Hu, D.-G.; Hao, Y.-J. Auxin regulates anthocyanin biosynthesis through the auxin repressor protein MdIAA26. *Biochem. Biophys. Res. Commun.* **2020**, *533*, 717–722. [[CrossRef](#)]
44. Wang, Y.-C.; Wang, N.; Xu, H.-F.; Jiang, S.-H.; Fang, H.-C.; Su, M.-Y.; Zhang, Z.-Y.; Zhang, T.-L.; Chen, X.-S. Auxin regulates anthocyanin biosynthesis through the Aux/IAA-ARF signaling pathway in apple. *Hortic. Res.* **2018**, *5*, 59. [[CrossRef](#)] [[PubMed](#)]
45. Clayton-Cuch, D.; Yu, L.; Shirley, N.; Bradley, D.; Bulone, V.; Böttcher, C. Auxin Treatment Enhances Anthocyanin Production in the Non-Climacteric Sweet Cherry (*Prunus avium* L.). *Int. J. Mol. Sci.* **2021**, *22*, 10760. [[CrossRef](#)] [[PubMed](#)]
46. Liu, Z.; Shi, M.-Z.; Xie, D.-Y. Regulation of anthocyanin biosynthesis in *Arabidopsis thaliana* red pap1-D cells metabolically programmed by auxins. *Planta* **2014**, *239*, 765–781. [[CrossRef](#)]
47. Qin, J.; Zhao, C.Z.; Wang, S.W.; Gao, N.; Wang, X.X.; Na, X.F.; Wang, X.M.; Bi, Y.R. PIF4-PAP1 interaction affects MYB-bHLH-WD40 complex formation and anthocyanin accumulation in *Arabidopsis*. *J. Plant Physiol.* **2022**, *268*, 153558. [[CrossRef](#)] [[PubMed](#)]
48. Feller, A.; Machemer, K.; Braun, E.L.; Grotewold, E. Evolutionary and comparative analysis of MYB and bHLH plant transcription factors. *Plant J.* **2011**, *66*, 94–116. [[CrossRef](#)] [[PubMed](#)]

49. Zheng, Y.; Jiao, C.; Sun, H.H.; Rosli, H.G.; Pombo, M.A.; Zhang, P.F.; Banf, M.; Dai, X.B.; Martin, G.B.; Giovannoni, J.J.; et al. iTAK: A Program for Genome-wide Prediction and Classification of Plant Transcription Factors, Transcriptional Regulators, and Protein Kinases. *Mol. Plant* **2016**, *9*, 1667–1670. [[CrossRef](#)]
50. Hu, J.T.; Chen, G.P.; Zhang, Y.J.; Cui, B.L.; Yin, W.C.; Yu, X.H.; Zhu, Z.G.; Hu, Z.L. Anthocyanin composition and expression analysis of anthocyanin biosynthetic genes in kidney bean pod. *Plant Physiol. Biochem.* **2015**, *97*, 304–312. [[CrossRef](#)]
51. Fang, S.Z.; Lin, M.; Ali, M.M.; Zheng, Y.P.; Yi, X.Y.; Wang, S.J.; Chen, F.X.; Lin, Z.M. LhANS-rr1, LhDFR, and LhMYB114 Regulate Anthocyanin Biosynthesis in Flower Buds of *Lilium* ‘Siberia’. *Genes* **2023**, *14*, 559. [[CrossRef](#)] [[PubMed](#)]

Disclaimer/Publisher’s Note: The statements, opinions and data contained in all publications are solely those of the individual author(s) and contributor(s) and not of MDPI and/or the editor(s). MDPI and/or the editor(s) disclaim responsibility for any injury to people or property resulting from any ideas, methods, instructions or products referred to in the content.